



# Temporal and spatial comparisons of ocean quahog (*Arctica islandica*) growth and lifespan on the mid-Atlantic continental shelf during inshore transgressions of their range from the Neoglacial through the twentieth century



Alyssa M. LeClaire <sup>a,\*</sup>, Eric N. Powell <sup>b</sup>, Roger Mann <sup>c</sup>, Kathleen M. Hemeon <sup>b,1</sup>, Sara M. Pace <sup>b</sup>, Vincent Saba <sup>d,e</sup>, Hubert du Pontavice <sup>b</sup>, Jillian R. Sower <sup>b</sup>

<sup>a</sup> CSS Inc Contracted to NOAA Beaufort Laboratory, 101 Pivers Island Rd, Beaufort, NC, 28516, USA

<sup>b</sup> Gulf Coast Research Laboratory, University of Southern Mississippi, 703 East Beach Drive, Ocean Springs, MS, 39564, USA

<sup>c</sup> Virginia Institute of Marine Science, College of William and Mary, 1370 Greate Rd, Gloucester Point, VA, 23062, USA

<sup>d</sup> Ecosystem Dynamics and Assessment Branch, NOAA Northeast Fisheries Science Center, Geophysical Fluid Dynamics Laboratory, Princeton University Forrestal Campus, 201 Forrestal Rd, Princeton, NJ, 08540, USA

<sup>e</sup> Princeton University, Atmospheric and Oceanic Sciences Program, 300 Forrestal Road, Sayre Hall, Princeton, NJ, 08540, USA

## ARTICLE INFO

### Keywords:

Ocean quahog  
*Arctica islandica*  
 Holocene  
 Growth rate  
 Northwestern atlantic  
 Neoglacial  
 Little ice age

## ABSTRACT

*Arctica islandica* provide long-term records of climate change on the U.S. northeast continental shelf transgressing and regressing across the shelf numerous times synchronously with cold and warm climatic periods. The availability of *A. islandica* in the death assemblage over a wide geographic and temporal range makes this species well suited for documenting both spatial and temporal influences of climate change in the Mid-Atlantic through the correlation of growth rates in response to changing water conditions. This study focuses on comparing regional growth of subfossil ocean quahogs obtained offshore of the Delmarva Peninsula (Delmarva), and living during the cold periods since the Holocene Climate Optimum, with living *A. islandica* from offshore New Jersey, offshore Long Island, and Georges Bank. These populations exhibited different growth rates, with subfossil individuals from Delmarva death assemblages, representing previous Holocene cold periods, having growth rates as greater than or equal the growth rates of living individuals. Moreover, the growth rates for subfossil *A. islandica* from Delmarva that were alive from 1740 to 1940 were more rapid than contemporaneous individuals of the same age alive today. Higher growth rates for *A. islandica* from off Delmarva suggest that conditions supported near maximum growth during the cold periods after the Holocene Climate Optimum, possibly due to increased food supply in water shallower than that inhabited today. Unlike many bivalves, evidence for range recession of *A. islandica* as bottom water temperatures warm is found first in juvenile abundance, suggesting that recruitment ceases long before the population's demise: range recession in this species is a 100+ year process determined by the survivorship of the oldest and largest individuals. This study is the largest spatial and temporal growth comparison of *A. islandica* ever recorded and the first record of the process by which this species' inshore range regresses as temperatures rise.

## 1. Introduction

Organism growth is controlled by ontogeny, genetics, and the environment (Hemeon et al., 2021a). Comparing growth over time between cohorts within and between populations allows one to isolate the effects

of a species' surrounding environments to determine the influence of environmentally-driven changes in growth (Black et al., 2008; Peharda et al., 2019; Hemeon et al., 2023a, b). By comparing temperature regimes and climatic events to known periods of growth, beneficial, neutral, or detrimental effects on growth can be inferred from

\* Corresponding author.

E-mail address: [alyssa.leclaire@noaa.gov](mailto:alyssa.leclaire@noaa.gov) (A.M. LeClaire).

<sup>1</sup> Current Affiliation: Abernathy Fish Technology Center, U.S. Fish and Wildlife Service, 1440 Abernathy Creek Rd, Longview, WA 98632, USA.

chronological growth increments recorded in the hard parts of an organism (Richardson, 2001; Killam and Clapham, 2018). For example, annual lines (annuli) deposited in the shells of bivalve molluscs (similar to the rings in a tree) capture a record of environmental information from the surrounding habitat (Peterson et al., 1985; Richardson, 2001; Kraeuter et al., 2007; Ridgway et al., 2011; Peharda et al., 2019). The distance between sequential annuli varies within a shell, recording the suitability of environmental conditions during each growth period. These annuli result from a changing rate of carbonate deposition during periods of slower or faster growth relative to the continuing deposition of organic matrix. Hence, the sampling of bivalves from a range of spatial, temporal, and environmental settings can provide consistent and accurate records of the individual's chronological age and local climate (Jones et al., 1984; Austad, 1996; Brey et al., 2011; Ridgway et al., 2011; Shirai et al., 2018).

*Arctica islandica*, commonly called the ocean quahog, is a boreal clam with a habitat range extending along the mid-Atlantic continental shelf and throughout most boreal seas in the northern hemisphere. Ocean quahogs have a well-known sensitivity to temperature, with an upper thermal limit of  $\sim 15$  °C, and an extensive lifespan often exceeding 300 years in age with the oldest aged at 507 years (Butler et al., 2013). These characteristics make *A. islandica* well suited for documenting the spatial and temporal influence of climate change, and previous investigations of this clam species span the majority of the North Atlantic, including the Mid-Atlantic region (Witbaard, 1996; Dahlgren et al., 2000; Witbaard and Bergman, 2003; Wanamaker et al., 2011; Butler et al., 2013; Reynolds et al., 2017; Hemeon et al., 2021a).

On the U.S. Mid-Atlantic continental shelf, *A. islandica* is found at latitudes farther south than the normal boreal provincial boundary (Hale, 2010). This unusual southern extension in range is a result of the Cold Pool, a body of cold bottom water trapped by thermal stratification during the late spring to early fall which maintains mean summer temperatures typically at 13.5 °C or lower, with fall temperatures rarely exceeding 16 °C when stratification breaks down (Lentz, 2017; Chen et al., 2018; Chen and Curchitser, 2020; Friedland et al., 2022).

As a result of the environmental information archived in the growth record of *A. islandica*, many studies have been conducted examining the determinants of growth in this long-lived species, with particular emphasis on temperature and food supply (Schöne et al., 2005; Wanamaker et al., 2009; Begum et al., 2010; Vihtakari et al., 2016; Balles-  
ta-Artero et al., 2017). Ocean quahogs are unique in their tendency for continuous growth into old age which limits the application of growth models that describe asymptotic growth at old age, typical of most bivalve species (e.g., McCuaig and Green, 1983; Devillers et al., 1998; Luquin-Cavarrubias et al., 2016). Hemeon et al. (2023a, b) determined that the best-fit growth model for ocean quahogs is a modified Tanaka model (MT) when compared to both the traditional Tanaka model (Tanaka, 1982; 1988) proposed by Pace et al. (2017a) and the von Bertalanffy model commonly used (e.g., Solidoro et al., 2000; Appleyard and DeAlteris, 2001; Kilada et al., 2009; Brey et al., 2011; Chute et al., 2016). The original Tanaka growth model, a power growth function, fits animals with indeterminate growth (Pace et al., 2017a), which is the case for ocean quahogs, but even so, it tends to underestimate growth of *A. islandica* at old age. Consequently, Hemeon et al. (2021a) modified the traditional Tanaka model (Tanaka 1982; Pace et al., 2017b) by adding an additional parameter, *g*, which permits the model to better estimate length at old age.

A primary objective of this study is to compare growth dynamics in existing and past ocean quahog populations from the U.S. Mid-Atlantic continental shelf. LeClaire et al. (2022) documented the presence of subfossil *A. islandica* shells in death assemblages sampled on the continental shelf off the Delmarva Peninsula inshore of the species' present depth range. These encompassed animals that lived during all four major cold events since the Holocene Climate Optimum (60–4400 cal years BP), including the two cold period events during the Neoglacial, the Dark Ages Cold Period, and the Little Ice Age. Given this spatial and

temporal distribution of ocean quahogs, LeClaire et al. (2022) proposed that the inshore boundary of the Cold Pool had transgressed and regressed across the continental shelf a number of times in the past and that during the transgressions associated with colder climates *A. islandica* occupied the inner to middle portion of the continental shelf inshore of their range today. The objective of this study is to compare the growth rates of subfossil ocean quahogs both spatially and temporally amongst themselves and with recently documented growth rates for living *A. islandica* obtained from three different regions in the U.S. Mid-Atlantic: New Jersey, Long Island, and Georges Bank (Hemeon et al., 2021a; Hemeon et al., in press; Sower et al., 2023b).

Notably, Pace et al. (2017b), Hemeon et al. (2023a, b), and Sower et al. (2022, 2023b) document the extraordinary variability in *A. islandica* growth rates as a function of birth year for *A. islandica* living in these Mid-Atlantic populations. Clams born in a given birth year integrate the subsequent climatology over their lifetimes, developing a growth curve that can differ from *A. islandica* born in other birth years. These differences document the sensitivity of the species to temperature change, a sensitivity that produces a differential growth dynamic based on the variance in temperature exposure for each cohort. Hence, comparisons can describe differences in growth over space and time, revealing the influence of biogeographic location and climate change on ocean quahog growth. Subsequent findings offer potential to identify the temperature history of the past populations alive during historical climate events, such as those identified by LeClaire et al. (2022), based on comparisons to extant populations.

## 2. Materials and methods

### 2.1. Sample processing

Growth data for living ocean quahogs were obtained from three different studies including animals collected off New Jersey (39°50.40'N, 72°49.20'W; Sower et al., 2023a), Georges Bank (40°43.66'N, 67°48.32'W; Hemeon et al., 2021a), and Long Island (40°5.95'N, 73°00.74'W; Hemeon et al., 2023a) in 2017 and 2019 (Fig. 1). Growth data from subfossil shells were obtained from locations reported by LeClaire et al. (2022), inshore and South of the Cold Pool (Figs. 1–3). The living ocean

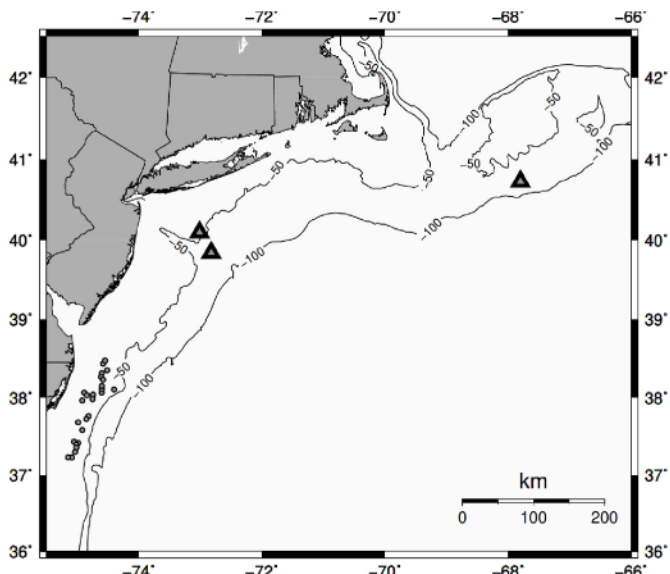


**Fig. 1.** Map of the *Arctica islandica* sample collection locations in the North-western Atlantic. Grey triangles represent locations where live ocean quahogs were collected offshore of Long Island, New Jersey, and Georges Bank. Grey circles represent subfossil ocean quahog collection sites from offshore of the Delmarva Peninsula, magnified in Fig. 2. Bathymetric contour depths in meters.

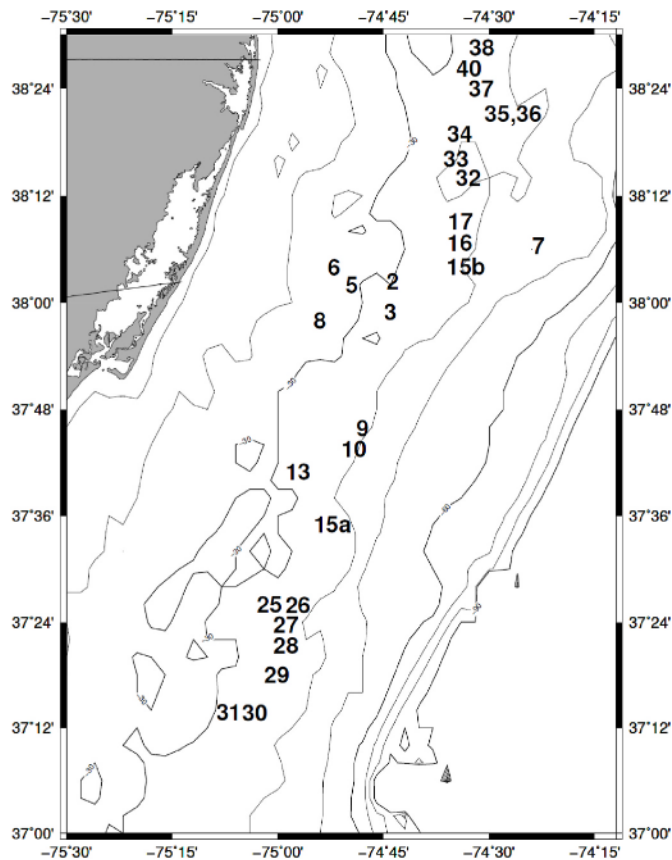


**Fig. 2.** Subfossil ocean quahog collection sites from offshore of the Delmarva Peninsula. Stations are identified as numbered during the survey. Bathymetric contour depths in meters. Additional details including the geographic distribution of shells of different times-since-death are provided by LeClaire et al. (2022).

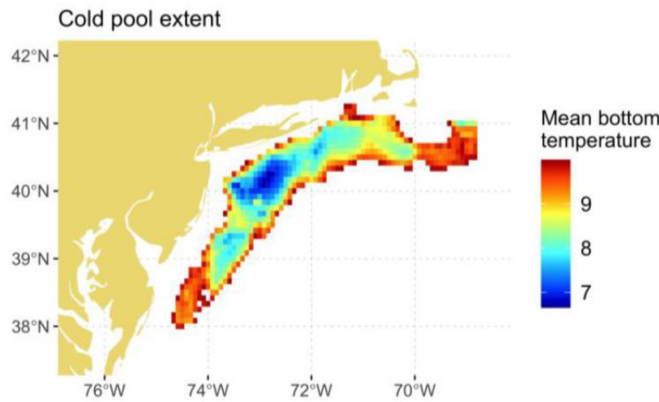


**Fig. 3.** Cold Pool extent for the period 1959–2021. The mean bottom temperature and extent were calculated using a high-resolution long-term bottom temperature product described in du Pontavice et al. (2023).

quahogs were collected within the extent of the Cold Pool between 1959 and 2021 (Fig. 3). Live and dead ocean quahogs were collected along the continental shelf using hydraulic dredges towed by commercial clam vessels. For live animals, a standard commercial ocean quahog hydraulic dredge was used (see Poussard et al., 2021). For subfossil collections, the dredge was lined with 1-inch-square wire on the bottom surface and knife shelf. Material collected by the dredge was sorted by clam species, live ocean quahog samples were shucked, and both live and subfossil

shells were retained and archived for later analysis. Samples selected from the archive were processed through a standard procedure described by Pace et al. (2017a) and Hemeon et al. (2021b). Each shell was cut along the maximum growth axis using a Kobalt wet tile saw. After being cut, shells were then ground using abrasive paper of increasing grit gauge (240, 320, 400, and 600) and polished with a polycrystalline diamond suspension fluid (6  $\mu$ m and 1  $\mu$ m diamond sizes) (Pace et al., 2017a; Hemeon et al., 2021b) to obtain a mirror finish. Shell hinges were imaged using a high-definition Olympus DP73 digital microscope camera. For subfossil shells and a subsample of live-collected shells (see LeClaire et al., 2022), after photographing the hinge, shell powder samples were extracted from the central portion of the interior edge of the shell near the hinge and umbo, using a Dremel tool to obtain carbonate that represented the youngest part of the shell hinge (i.e., carbonate deposited during the earliest growth). The powder sample ( $>10$  mg) was sent to the W. M. Keck Carbon Cycle Accelerator Mass Spectrometry Laboratory at the University of California, Irvine for analysis. Radiocarbon dates were calibrated according to the methods in LeClaire et al. (2022).

## 2.2. Aging

Following the methods described in Pace et al. (2017a), images of the shell hinge plate were annotated using ImageJ software to estimate age. Reader precision was evaluated using the double-blind technique of Hemeon et al. (2021b) who provide a detailed evaluation of reader precision in the aging of *A. islandica* also applicable to this study. Accuracy was evaluated by comparing radiocarbon dated specimens of known date-of-death with reader ages as described by LeClaire et al. (2022). Annual growth increments were measured in pixels by the ObjectJ plugin for ImageJ (Pace et al., 2018; Hemeon et al., 2021b). Annual lines observed on the shell hinge plate are proportional to increments on the outer shell valve (Mann, unpubl. data); therefore, annual growth increments on the hinge plate were converted to annual growth increments of the total shell length using the ratio of the hinge plate length to total length after conversion of pixel dimension to mm (Pace et al., 2018; Hemeon et al., 2021b). Supplementary information on *A. islandica* shell processing procedures can be found at: [https://www.vims.edu/research/units/labgroups/molluscan\\_ecology/publications/topic/ocean\\_quahog\\_arctica/index.php](https://www.vims.edu/research/units/labgroups/molluscan_ecology/publications/topic/ocean_quahog_arctica/index.php).

### 2.2.1. Growth model

The growth increments for each shell were cumulatively summed to create a growth curve for that specific individual. Using the Akaike information criterion (AIC), Hemeon et al. (2021a) determined that the modified Tanaka model (MT) was the best-fit growth model for ocean quahog growth (Eq (1)):

$$L_t = d + \frac{1}{\sqrt{f}} \log \left( 2f(t - c) + 2\sqrt{f^2(t - c)^2 + fa} \right) + gt^{2.5} \quad (1)$$

where  $L_t$  is the shell length in mm at a given age in years (t). The MT model parameters can be understood as follows. Parameter  $c$  (yr) denotes the age at maximum growth rate. At the age of maximum growth,  $c$ , the growth rate is  $1/\sqrt{a}$ . Therefore, parameter  $a$  ( $\text{yr}^2 \text{mm}^{-2}$ ) describes the maximum growth rate which will occur at age  $c$ . Parameter  $f$  ( $\text{yr}^{-2}$ ) controls the rate at which growth declines with increasing age. For older animals, growth rate reduces to  $1/(t\sqrt{f})$ . Parameters  $d$  (mm) and  $g$  ( $\text{mm yr}^{-2.5}$ ) are scalers of size, with  $g$  influencing the rate of growth rate decline with increasing age determined by parameter  $f$ . All MT model parameters except  $d$ , were forced to be  $\geq 0$  during model convergence to prevent the estimation of negative square roots and logarithms.

For comparison with data from Hemeon et al. (2021a, 2023b) and Sower et al. (2023b), dead shells reported in LeClaire et al. (2022) that were born after 1700 were divided into 20-year groups defined by birth year.

### 2.3. Death dates

The age-at-death of each subfossil shell collected off Delmarva and reported in LeClaire et al. (2022) was added to the radiocarbon age (assumed to approximate the birth year of the animal), to determine the year of death.

### 2.4. Temperature model

Using data from Hemeon et al. (2021a, 2023a), animals collected from Georges Bank and Long Island were compared to bottom water temperatures for these collection locations. Bottom temperature data were obtained from the simulations of the Northwest Atlantic Ocean in the Regional Ocean Modelling System (ROMS-NWA; Shchepetkin and McWilliams, 2005) for the period 1959–1992 and from the Global Ocean Physics Reanalysis (Glorys12v1 reanalysis; Lellouche et al., 2021) for the period 1993–2017. Based on the methodology developed by du Pontavice et al. (2022), bottom temperature from ROMS-NWA used for the period 1959–1992 were bias-corrected using the monthly climatologies of observed bottom temperature from the Northwest Atlantic Ocean regional climatology (NWARC) (Seidov et al., 2016). The extent of the Cold Pool was estimated between 1959 and 2021 (Fig. 3) calculated using a high-resolution long-term bottom temperature product described in du Pontavice et al. (2023).

A generalized additive model (GAM) was fit to the yearly maximum values obtained from the bottom temperature dataset compared to the yearly growth of animals to describe the relationship between growth and temperature. Several temperature metrics were investigated; yearly maximum temperature was determined to have the largest and most significant effect on growth. The majority of temperatures between 1958 and 2017 fall within the range of temperatures that ocean quahogs are able to tolerate (5–15 °C). Consequently, using the maximum temperature enabled a focus on the temperatures at the edge or outside of this clam's temperature tolerance. The GAMs were fit in R Statistical Software (v4.1.2; R Core Team 2021) using the mgcv package (v1.8-34; Wood, 2011). Growth was the response variable with maximum yearly temperature, sex, location, and animal age in that growth year used as predictor variables to explain the differences in growth. The model was tested with `gam.check()` to determine the appropriate number of basis functions, consequently setting the number for maximum temperature and age to 15 ( $k = 15$ ):

$$\text{rowth Increment} = s(\text{maximum tempurature}, k = 15) + s(\text{age}, k = 15) + \text{sex} + \text{location} \quad (2)$$

Model variables were also checked for collinearity using the `concurvity()` function and determined not to be strongly correlated to one another.

## 3. Results

Comparison of the MT growth curves for the subfossil shells collected off Delmarva with birth dates contemporaneous with living animals from New Jersey, Long Island, and Georges Bank born after 1700 CE showed that the subfossil ocean quahogs from Delmarva grew faster than those from all other regions, with animals from Georges Bank representing the second fastest growth rates (Fig. 4). Growth curves from Long Island and New Jersey were extremely similar at young and middle ages, but older New Jersey animals were larger than Long Island animals at the same age (Fig. 4). When comparing populations with contemporaneous birth dates (1700–2017 CE) from Georges Bank, Long Island, New Jersey, and Delmarva, maximum growth rate (i.e., smaller  $a$ ) was highest for Delmarva (Table 1), followed by Georges Bank and then by New Jersey and Long Island. The age at maximum growth rate ( $c$ ), was youngest at Georges Bank, with Long Island, New Jersey and

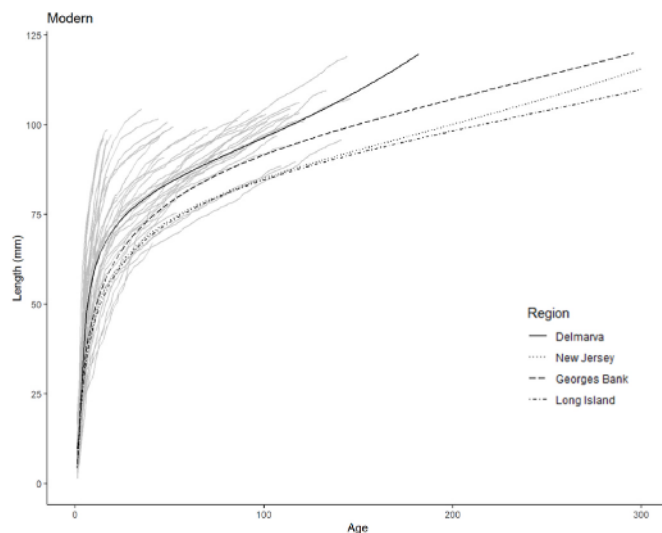


**Fig. 4.** Growth curves for animals with birth dates contemporaneous with living ocean quahogs collected from the Mid-Atlantic continental shelf. Black lines represent Modified Tanaka growth curves for ocean quahogs born after 1700 BCE compared across regions. Average growth curves for subfossil shells from Delmarva (solid line) and living animals from New Jersey (dotted line), Georges Bank (dashed line), and Long Island (dot-dashed line) are presented along with individual growth curves for each animal in the subfossil Delmarva sample (light grey lines).

Delmarva demonstrating increasing age at maximum growth rate (Table 2). All of these ages at maximum growth fell within the first 4 years of life, however. The rate of decline of growth rate with age was lowest at Delmarva (higher  $f$ ), then New Jersey, Long Island, and Georges Bank. A scale of body size, ( $d$ ) was largest at Georges Bank, then Delmarva, Long Island, and New Jersey (Table 1).

Fig. 5 depicts temporal and spatial trends in growth from 1740 to 1940 CE at Delmarva, Georges Bank, and Long Island respectively broken into 20-yr groupings by birthdate. Parameter values are provided in Table 2. The New Jersey population was not grouped as growth rates were similar to Long Island and as a result was excluded from Fig. 5. Without exception, growth rates for the vicennial groups were as high or higher for the subfossil Delmarva shells than for live-collected animals from Long Island and Georges Bank.

Modified Tanaka growth curves (Fig. 6) for animals born during major climate events in the Holocene illustrate the temporal changes in growth during these major events including the Little Ice Age (LIA) (207–462 cal years BP), Medieval Warm Period (MWP) (877 cal years BP), Dark Ages Cold Period (DACP) (1167–1223 cal years BP), Roman Warm Period (RWP) (2447 cal years BP), Neoglacial part 1 (Neo1) (2813–3093 cal years BP), Neoglacial part 2 (Neo2) (3418–3542 cal years BP), and the Meghalayan stage boundary (Meg) (3817–4302 cal years BP). For more on these time periods, see Wanner et al. (2011), Auger et al. (2019), and LeClaire et al. (2022). Parameter values for the Modified Tanaka growth curves for each of these time periods are provided in Table 3. The growth of subfossil ocean quahogs collected from Delmarva was always greater than or equal to the growth of ocean quahogs from Long Island, Georges Bank, and New Jersey, regardless of the time period in which they lived. Growth was fastest during the Roman Warm Period and the Dark Ages Cold Period, followed by the Medieval Warm Period. Growth during the Meghalayan stage boundary was almost the same as during the earliest part of the Neoglacial, with the late Neoglacial shells growing slightly faster. Almost no difference is present during Neo1 and Neo2 while the differences are substantial during the Dark Ages Cold Period and Roman Warm Period. Growth during the Little Ice Age and between 1740 and 1960 CE were very similar.

**Table 1**

Modified Tanaka growth parameters (Eq. (1)) from living populations from Georges Bank, Long Island, and New Jersey, and the subfossil Delmarva animals with contemporaneous birth dates.

Group	Parameter	Georges Bank		Long Island		New Jersey		Delmarva	
		Estimate	SE	Estimate	SE	Estimate	SE	Estimate	SE
Contemporary Population	<i>a</i>	7.36E-03	7.34E-04	1.57E-02	7.29E-04	1.69E-02	6.07E-04	7.91E-03	9.17E-04
	<i>c</i>	7.62E-01	7.62E-02	1.77 E+00	6.88E-02	2.40 E+00	6.55E-02	3.76 E+00	1.72E-01
	<i>d</i>	8.78 E+01	2.03E-01	7.73 E+01	1.53E-01	7.61 E+01	1.62E-01	8.00 E+01	8.41E-01
	<i>f</i>	3.00E-03	2.82E-05	3.90E-03	3.48E-05	4.34E-03	4.30E-05	6.99E-03	4.21E-04
	<i>g</i>	6.04E-06	4.29E-07	5.07E-06	2.66E-07	9.34E-06	3.86E-07	4.59E-05	5.68E-06

**Table 2**

Modified Tanaka growth parameters and standard error (SE) for 20-year groupings by birth for Georges Bank (GB), Long Island (LI), and the subfossil Delmarva animals of contemporaneous birth dates.

Cohort	Parameter	Georges Bank Population		Long Island Population		Delmarva Population	
		Estimate	SE	Estimate	SE	Estimate	SE
1740	<i>a</i>	6.55E-03	9.64E-03	9.91E-03	9.63E-03	8.54E-03	5.13E-03
	<i>c</i>	0.00 E+00	8.07E-01	0.00 E+00	5.85E-01	2.94 E+00	1.03 E+00
	<i>d</i>	8.10 E+01	1.45 E+00	7.09 E+01	7.68E-01	8.72 E+01	4.89 E+00
	<i>f</i>	2.19E-03	1.34E-04	2.91E-03	1.26E-04	4.60E-03	1.21E-03
	<i>g</i>	9.14E-06	1.01E-06	1.46E-05	5.97E-07	7.29E-06	2.76E-05
1760	<i>a</i>			4.46E-02	2.83E-02	7.21E-03	1.41E-03
	<i>c</i>			0.00 E+00	1.22 E+00	2.96 E+00	2.75E-01
	<i>d</i>			7.36 E+01	1.29 E+00	7.99 E+01	1.22 E+00
	<i>f</i>			2.56E-03	1.76E-04	6.52E-03	5.63E-04
	<i>g</i>			1.58E-05	9.69E-07	3.08E-05	6.19E-06
1780	<i>a</i>	1.14E-02	6.26E-03	1.46E-02	8.31E-03	3.15E-03	2.99E-03
	<i>c</i>	0.00 E+00	4.09E-01	0.00 E+00	4.77E-01	1.50 E+00	8.12E-01
	<i>d</i>	8.42 E+01	6.49E-01	6.98 E+01	6.71E-01	1.03 E+02	4.56 E+00
	<i>f</i>	2.61E-03	8.21E-05	2.84E-03	1.01E-04	2.94E-03	5.23E-04
	<i>g</i>	7.67E-06	6.34E-07	2.02E-05	6.73E-07	0.00 E+00	1.49E-05
1800	<i>a</i>	5.74E-03	6.39E-03	1.33E-02	5.85E-03	8.08E-03	1.05E-03
	<i>c</i>	0.00 E+00	5.14E-01	0.00 E+00	3.52E-01	2.42 E+00	2.20E-01
	<i>d</i>	8.78 E+01	1.01 E+00	7.24 E+01	5.46E-01	9.22 E+01	1.17 E+00
	<i>f</i>	2.53E-03	1.15E-04	2.83E-03	7.92E-05	3.73E-03	1.97E-04
	<i>g</i>	6.91E-06	1.17E-06	2.10E-05	6.53E-07	3.64E-05	6.29E-06
1820	<i>a</i>	9.56E-03	4.31E-03	2.50E-02	9.59E-03	1.04E-02	1.60E-03
	<i>c</i>	0.00 E+00	3.24E-01	0.00 E+00	4.73E-01	3.48 E+00	2.86E-01
	<i>d</i>	8.95 E+01	6.58E-01	7.54 E+01	6.61E-01	8.42 E+01	1.36 E+00
	<i>f</i>	2.41E-03	6.72E-05	2.99E-03	1.07E-04	5.73E-03	4.83E-04
	<i>g</i>	9.31E-06	8.87E-07	2.49E-05	9.34E-07	2.95E-05	8.94E-06
1840	<i>a</i>	9.48E-03	4.35E-03	4.37E-03	4.27E-03	1.31E-02	3.02E-03
	<i>c</i>	2.64E-01	3.63E-01	0.00 E+00	3.12E-01	2.63 E+00	4.63E-01
	<i>d</i>	9.11 E+01	8.51E-01	7.77 E+01	6.29E-01	8.59 E+01	1.85 E+00
	<i>f</i>	2.52E-03	8.96E-05	3.21E-03	1.04E-04	3.90E-03	3.57E-04
	<i>g</i>	9.38E-06	1.50E-06	2.60E-05	1.24E-06	3.53E-05	7.55E-06
1860	<i>a</i>	1.12E-02	2.63E-03	4.62E-03	3.72E-03	1.55E-02	6.00E-03
	<i>c</i>	9.50E-01	2.62E-01	1.51E-01	3.05E-01	2.77 E+00	9.63E-01
	<i>d</i>	8.82 E+01	7.35E-01	8.00 E+01	7.24E-01	8.98 E+01	4.74 E+00
	<i>f</i>	2.91E-03	9.38E-05	3.16E-03	1.11E-04	3.67E-03	7.63E-04
	<i>g</i>	1.91E-05	1.87E-06	3.13E-05	1.78E-06	0.00 E+00	2.97E-05
1880	<i>a</i>	1.01E-02	1.67E-03	1.43E-02	3.30E-03	3.60E-03	1.32E-03
	<i>c</i>	1.08 E+00	1.84E-01	8.66E-01	2.89E-01	2.20 E+00	9.14E-01
	<i>d</i>	8.69 E+01	5.93E-01	8.33 E+01	8.02E-01	1.58 E+02	2.41 E+01
	<i>f</i>	3.11E-03	8.17E-05	2.99E-03	1.06E-04	1.36E-03	5.30E-04
	<i>g</i>	1.79E-05	2.04E-06	3.01E-05	2.59E-06	0.00 E+00	9.72E-04
1940	<i>a</i>	1.06E-02	9.45E-04	1.25E-02	5.62E-04	1.70E-02	3.78E-02
	<i>c</i>	2.21 E+00	1.65E-01	2.74 E+00	9.12E-02	0.00 E+00	6.27 E+01
	<i>d</i>	8.31 E+01	9.85E-01	7.39 E+01	5.22E-01	7.14 E+02	2.65 E+03
	<i>f</i>	4.27E-03	1.93E-04	5.60E-03	1.63E-04	7.03E-05	5.00E-04
	<i>g</i>	7.39E-05	1.30E-05	9.39E-05	8.46E-06	0.00 E+00	1.18E-02

SE, standard error.

Subfossil shells from Delmarva lived to between 16 and 247 years of age (Fig. 7), an age range similar to that recorded for present-day living populations by Hemeon et al. (2021a, 2023a) and Sower et al. (2023a). Age-at-death was well distributed across radiocarbon birth years between 60 and 4400 years ago (Fig. 7), suggesting little variability in age-at-death within this admittedly small sample size. Analyzing the subfossil Delmarva *A. islandica* that died in the past 200 years, younger animals became less common closer to present time, with their near

disappearance starting about 120 years before present (Fig. 8).

The generalized additive model (GAM) showed a negative relationship between the annual maximum temperature of the Cold Pool at the Long Island and Georges Bank collection locations and the growth of *A. islandica* living there during the 1958–2017 time period (Fig. 9). The ANOVA (conducted via the summary () function) verified the smooth terms (maximum temperature and age) and parametric coefficients (sex and location) used in the GAM (Eq (2)) were all significant ( $p < 2e^{-16}$ ),

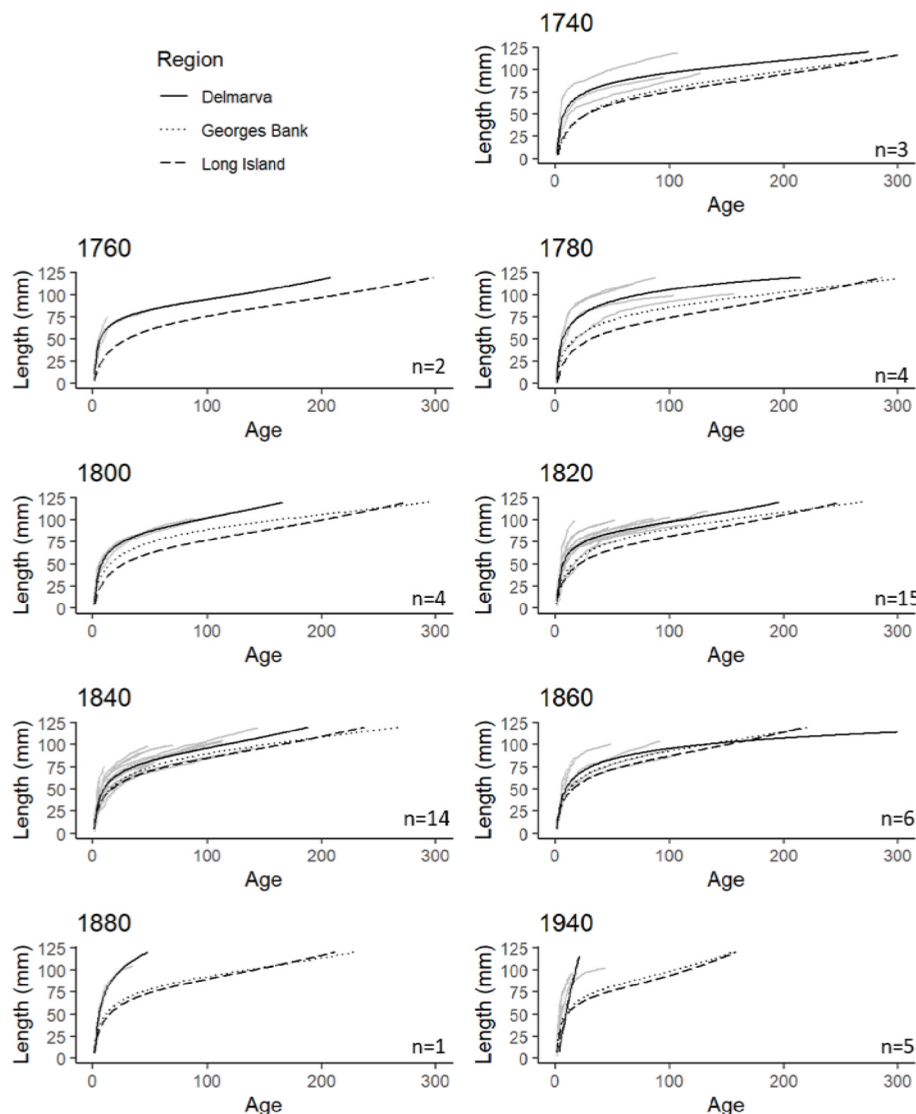


**Fig. 5.** Growth curves for 20-yr groups defined by birthdate for ocean quahogs born since 1700. Black lines represent average Modified Tanaka curves compared across regions and 20-year groupings by birth date including subfossil shells from Delmarva (solid line) and living animals from Long Island (dashed line) and Georges Bank (dotted line). Light grey lines represent the individual growth curves for each animal in the subfossil contemporaneous Delmarva sample.

explaining 40.3% of the deviance ( $R^2 = 0.403$ ). Results are consistent with the known differential in growth rate between Long Island and Georges Bank (Hemeon et al., 2023b), and the well-established dimorphism between the growth rate of males and females (Hemeon et al., 2023a; Sower et al., 2022; 2023a). The GAM revealed a modest downward trend in growth rate across the temperature range of 10–15 °C, but a substantial decline as maximum temperature exceeded 15 °C, consistent with the known thermal limit for ocean quahogs of ~16 °C.

#### 4. Discussion

##### 4.1. Regional and temporal comparisons in growth rates

The growth models change over time between the 20-yr groupings, with growth rates at age increasing from the mid-to-late 19<sup>th</sup> century into the 20<sup>th</sup> century as reported by Hemeon et al. (2021a, 2023b) and Sower et al. (2022, 2023b). Regional differences in growth rate of ocean quahogs were also observed for living *A. islandica* across the three study regions. As Hemeon et al. (2023b) reported, Georges Bank *A. islandica* exhibit faster growth rates than Long Island. As observed by Sower et al. (2023b), growth of ocean quahogs from New Jersey and Long Island had

very similar rates, nearly identical until animals reached an old age (Fig. 4, Table 1).

The growth models show different growth rates for these living populations and the subfossil *A. islandica* from Delmarva with contemporary birth dates as well as older Delmarva clams from earlier Holocene cold climate events. Unexpectedly, Delmarva subfossil ocean quahogs collected inshore of the present-day distribution of the species grew as fast or faster than animals from these other studied regions. Previous to this study, both Hemeon et al. (2023b) and Pace et al. (2018) found ocean quahogs from Georges Bank to have the highest growth rates in the Mid-Atlantic among living populations so far studied; however, even growth rates at Georges Bank were equaled or exceeded by growth rates obtained from subfossil shells off Delmarva in this study.

Delmarva subfossil ocean quahogs born post-1700 had equal or higher growth rates compared to living animals born after 1700 from all three regions, and this higher rate of growth was consistently present regardless of vicennial birth group. Continuously higher growth rates for the population born between 1740 and 1960 inshore off Delmarva support the inference that the Delmarva populations lived under conditions that may have maximized growth prior to the demise of this population which likely was concluded in the 1970s. Additionally, the

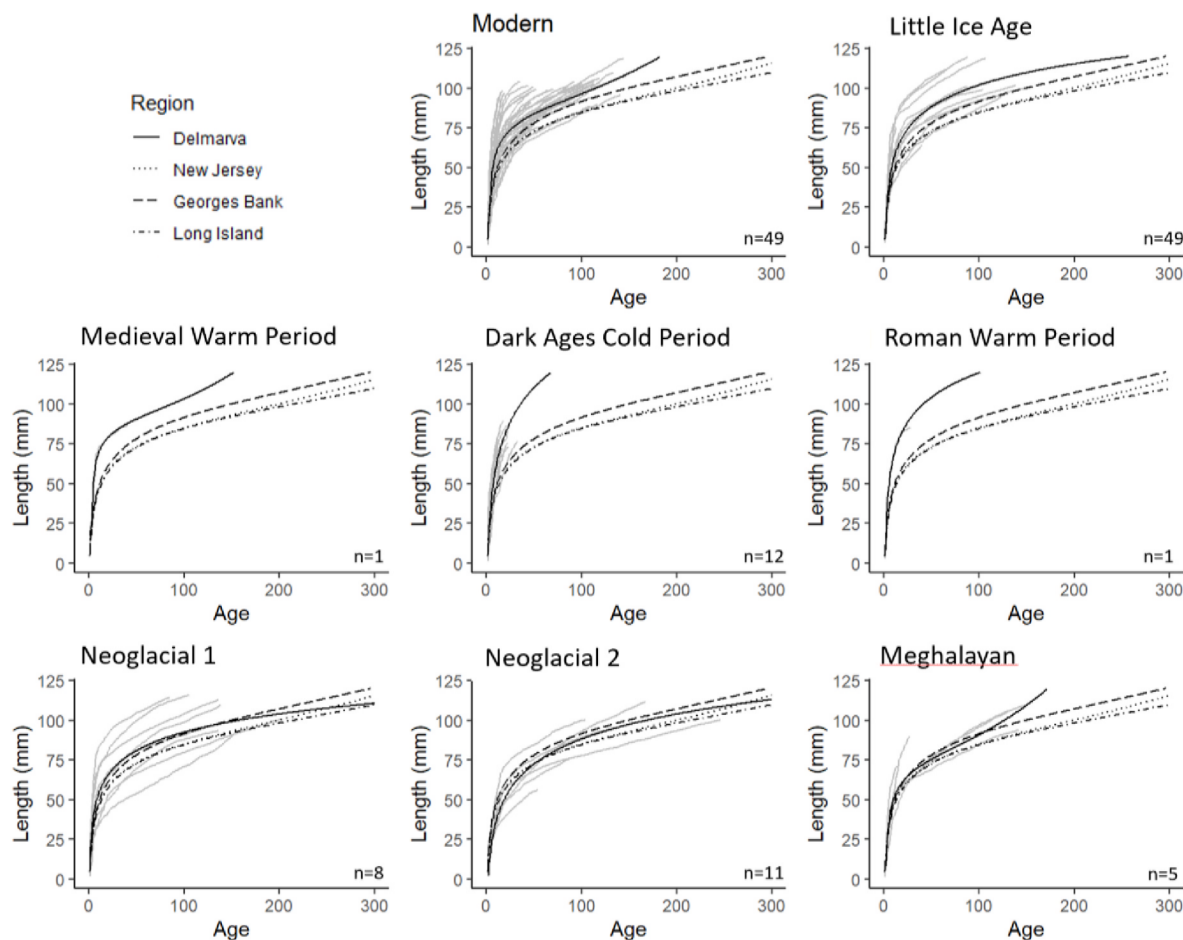


**Fig. 6.** Growth curves for ocean quahogs born during selected time intervals of the Holocene. Black lines represent average Modified Tanaka growth curves for subfossil shells born off Delmarva during major climate events in the Holocene: Modern (60–203 cal years BP), Little Ice Age (207–462 cal years BP), Medieval Warm Period (877 cal years BP), Dark Ages Cold Period (1167–1223 cal years BP), Roman Warm Period (2447 cal years BP), Neoglacial part 1 (2813–3093 cal years BP), Neoglacial part 2 (3418–3542 cal years BP), Meghalayan stage boundary (3817–4302 cal years BP). Solid lines represent the average growth curve for subfossil shells sampled off the Delmarva Peninsula. Curves from New Jersey, Georges Bank, and Long Island represent living animals born after 1700 (Modern) and used for comparison in the graphs depicting growth during the Holocene climate events. The dotted line represents the growth for living *A. islandica* off the coast of New Jersey, the long dashes represent Georges Bank, and the dot-dash line represents Long Island. Light grey lines represent the individual growth curves for each animal in the subfossil Delmarva sample born in the designated climate period.

differences between growth curves during the major climate events in the Holocene predict a period for optimal growth between Medieval Warm Period and Roman Warm Period (Fig. 6). During the Long Island Age, the growth curves are similar compared to the modern period (except for animals at old age) while animals living during Medieval and Roman Warm Period had growth rates much greater than in the other periods and regions (Fig. 6). These observed higher growth rates for subfossil populations off Delmarva suggest that environmental conditions supporting optimal growth were present during the lifetime of these clams. Presumably, bottom temperatures supported maximum growth before reaching intolerable levels that eventually led to the death of all inshore ocean quahogs prior to the 1980s (Figs. 8 and 9).

#### 4.2. Why were growth rates so high during past cold periods?

For most bivalves, including *A. islandica*, growth rates increase with increasing temperature until an optimal temperature is exceeded and growth rates decline. This parabolic relationship of physiology and temperature is well described (Woodin et al., 2013) and physiologically based in the relationship of filtration rate and respiration rate in bivalves: the two metabolic energetic processes that are primary determinants of scope for growth (Ren and Ross, 2001; Hofmann et al., 2006; Munroe et al., 2013). The GAM model (Fig. 9) shows the influence

of present-day yearly maximum temperatures at the Long Island and Georges Bank sites, with a clear break point at 15 °C. This temperature is often exceeded for periods during the early fall when water-column stratification breaks down, the increasing frequency of which being a product of the rapid warming of this region of the Mid-Atlantic (Lucey and Nye, 2010; Pershing et al., 2015; Saba et al., 2016; Kavanaugh et al., 2017). Presumably, present-day high temperatures cause *A. islandica* growth to slow either due to a physiological constraint or to a cessation of feeding due to estivation to escape the highest temperatures when the Cold Pool decays in the early fall. Burrowing behavior in the species is well described (Ragnarsson and Thorarinsdottir, 2002; Strahl et al., 2011) and the species can survive without oxygen for extended periods of time (Taylor, 1976a, 1976b; Oeschger and Storey, 1993). Whether due to physiological constraints or estivation, the growing season is effectively shortened. If such extreme conditions were present for subfossil shells off Delmarva, one would not expect to observe the higher growth rates consistently present for Delmarva animals relative to rates observed for living animals from Long Island and Georges Bank.

Accordingly, one could infer that increased temperatures relative to today seem an unlikely explanation for the increased growth rate, and this is further supported by the fact that growth rates for dead *A. islandica* born in the 19<sup>th</sup> and early 20<sup>th</sup> century off Delmarva are higher than contemporaneous clams still living at Long Island and

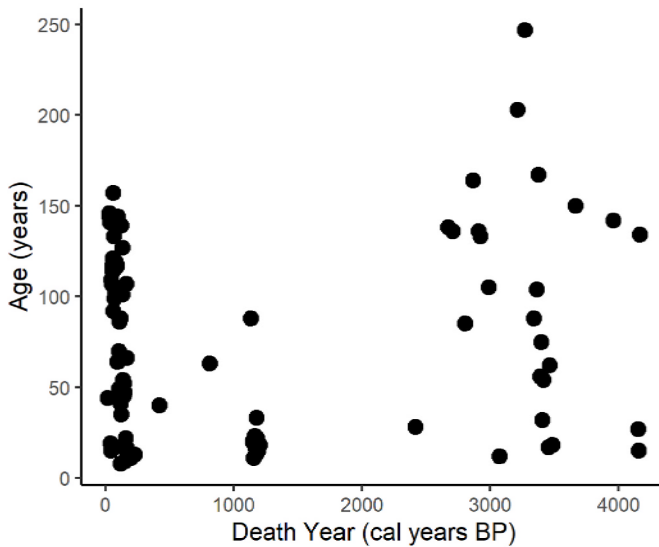
**Table 3**

Modified Tanaka model parameters for subfossil shells from Delmarva grouped by climate event before present time (BP), including the Little Ice Age (207–462 cal years BP), Medieval Warm Period (877 cal years BP), Dark Ages Cold Period (1167–1223 cal years BP), Roman Warm Period (2447 cal years BP), Neoglacial part 1 (2813–3093 cal years BP), Neoglacial part 2 (3418–3542 cal years BP), and the Meghalayan stage boundary (3817–4302 cal years BP).

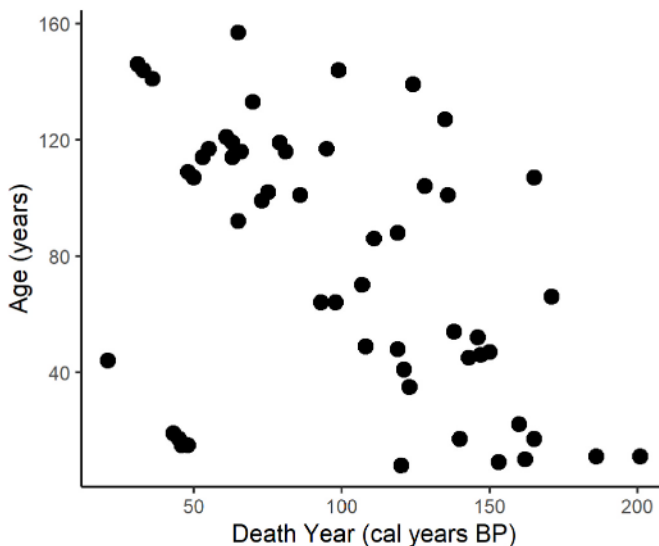
Climate Event	Parameter	Delmarva	
		Estimate	SE
Modern	<i>a</i>	7.91E-03	9.17E-04
	<i>c</i>	3.76 E+00	1.72E-01
	<i>d</i>	8.00 E+01	8.41E-01
	<i>f</i>	6.99E-03	4.21E-04
	<i>g</i>	4.59E-05	5.68E-06
	<i>a</i>	8.77E-03	4.07E-03
Little Ice Age	<i>c</i>	1.74 E+00	6.79E-01
	<i>d</i>	1.00 E+02	2.98 E+00
	<i>f</i>	2.79E-03	3.20E-04
	<i>g</i>	0.00 E+00	1.02E-05
	<i>a</i>	3.89E-03	6.43E-04
	<i>c</i>	4.10 E+00	1.19E-01
Medieval Warm Period	<i>d</i>	8.32 E+01	1.14 E+00
	<i>f</i>	1.02E-02	8.89E-04
	<i>g</i>	6.67E-05	3.41E-05
	<i>a</i>	1.03E-03	7.28E-03
	<i>c</i>	0.00 E+00	2.57 E+00
	<i>d</i>	1.59 E+02	4.74 E+01
Dark Ages Cold Period	<i>f</i>	1.04E-03	7.05E-04
	<i>g</i>	0.00 E+00	2.03E-03
	<i>a</i>	4.17E-03	1.81E-03
	<i>c</i>	1.60 E+00	8.25E-01
	<i>d</i>	1.23 E+02	1.74 E+01
	<i>f</i>	2.18E-03	8.41E-04
Roman Warm Period	<i>g</i>	0.00 E+00	1.19E-03
	<i>a</i>	3.53E-03	5.72E-03
	<i>c</i>	1.01 E+00	8.77E-01
	<i>d</i>	8.60 E+01	2.69 E+00
	<i>f</i>	3.75E-03	5.43E-04
	<i>g</i>	0.00 E+00	6.41E-06
Neoglacial Part 1	<i>a</i>	3.67E-03	9.30E-03
	<i>c</i>	0.00 E+00	1.02 E+00
	<i>d</i>	9.36 E+01	2.77 E+00
	<i>f</i>	1.97E-03	1.89E-04
	<i>g</i>	0.00 E+00	2.80E-06
	<i>a</i>	1.11E-02	2.93E-03
Neoglacial Part 2	<i>c</i>	3.24 E+00	4.49E-01
	<i>d</i>	7.16 E+01	1.58 E+00
	<i>f</i>	6.61E-03	7.83E-04
	<i>g</i>	7.74E-05	7.33E-06
	<i>a</i>	1.11E-02	2.93E-03
	<i>c</i>	3.24 E+00	4.49E-01
Meghalayan	<i>d</i>	7.16 E+01	1.58 E+00
	<i>f</i>	6.61E-03	7.83E-04
	<i>g</i>	7.74E-05	7.33E-06

Georges Bank. Yet, evidence clearly indicates that growth rates for Long Island and Georges Bank were lower in the 19<sup>th</sup> century than observed today (Pace et al., 2018; Hemeon et al., 2023a). Consequently, a simple increase in temperature appears insufficient to support the observed higher growth rates for subfossil shells collected off Delmarva that lived throughout the Holocene. Shells from ocean quahogs spawned during most cold and warm events during the Holocene were growing as fast or at faster rates than the present populations in Georges Bank, Long Island, and New Jersey.

Increases in food supply also produce increasing rates of growth (Schöne et al., 2005; Mette et al., 2016; Ballesta-Artero et al., 2017). As the fast rate of growth for subfossil Delmarva shells indicates that conditions off Delmarva were most suitable for growth for the resident *A. islandica* population at that time, and that increased temperature was a necessary, but not a sufficient, explanation, an additional increased food supply would seem to be a co-occurring requisite. Little is known about the influence of warming temperatures on phytoplankton production in the studied region (Friedland et al., 2018; 2020b), though considerable attention has been given to the influence of warming temperatures on phytoplankton production in general (e.g., Oviatt, 2004; Richardson and Schoeman, 2004; Osman et al., 2019; Lotze et al., 2019). In particular, detailed knowledge of the influence of the

**Age vs Death**

**Fig. 7.** Age-at-death of subfossil ocean quahogs compared to the time (death year) that the animal died. Death years are in years before present, focusing on animals that died between 62 and 4400 years ago.

**Age vs Death**

**Fig. 8.** Age of subfossil ocean quahogs at death compared to the time (death year) that the animal died. Death years are in years before present, focusing on animals that died in the past 200 years.

inshore-offshore depth gradient on phytoplankton production is limited in the studied region (Yoder et al., 2002; Mouw and Yoder, 2005; Munroe et al., 2013). Despite the lack of studies, phytoplankton production has been shown to be insufficient to meet the food supply requirements of the largest bivalve in the region, the Atlantic surfclam *Spisula solidissima* (Munroe et al., 2013). Munroe et al. (2013) argue that benthic primary production is a critical supplement to phytoplankton production to support biomass of the Atlantic surfclam on the Mid-Atlantic continental shelf.

Whereas not enough is known about the food requirement of ocean quahogs to blithely extrapolate from the surfclam case, the subfossil ocean quahogs with radiocarbon dates from known cold periods since the Holocene Climate Optimum were collected at study sites off Delmarva with depths considerably shallower than the present range of this

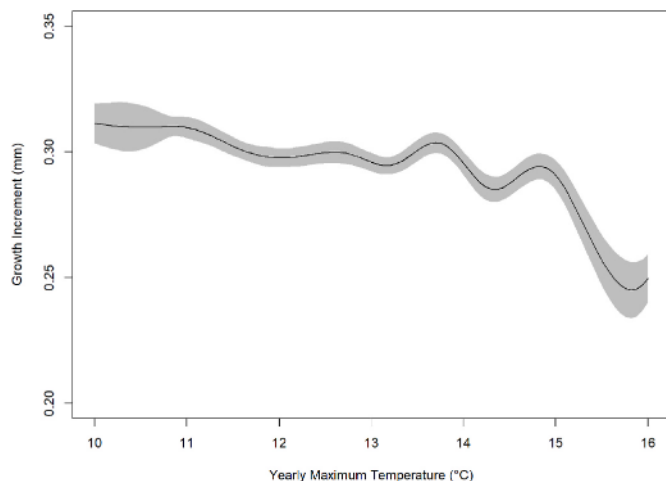


**Fig. 9.** General additive model of yearly growth increment as a function of yearly maximum temperature between 1958 and 2017 (ROMS-NWA; du Pontavice et al., 2022). Grey bar represents the 95% confidence interval surrounding the GAM.

species south of Long Island. Sea level at the earliest cold times recorded by the Delmarva animals was slightly lower than today (Engelhart et al., 2011), indicating animals would have lived at depths even shallower than presently recorded depths at these sites. *Artica islandica* have no shallow-water depth restriction, and are found at much shallower depths than those off Delmarva, including locations well inshore off Long Island, as well as elsewhere in the North Atlantic (Zettler et al., 2001; Ragnarsson and Thorarinsdottir, 2002; Strahl et al., 2011; Begum et al., 2019). Hence, the depth range of past occupation off Delmarva is not unusual for the species. Shallow depths are higher in the photic zone where benthic primary production is enhanced (Munroe et al., 2013) permitting speculation that the increased growth rates observed were due not only to optimal thermal conditions, but also to greater food availability.

#### 4.3. The dynamics of range recession in ocean quahogs

Ocean quahog growth at Georges Bank was comparable to growth off Delmarva during early Holocene cold periods (Meg and Neo1,2) and somewhat slower than subsequent cold periods (the DACP and LIA). Throughout the Meghalayan and Neoglacial, the Delmarva growth curves are similar to those of the living Georges Bank populations in the modern period (Fig. 6) suggesting that thermal conditions during the Neoglacial were similar to those in Georges Bank after 1700. Notably, the distribution of the Delmarva subfossil shells strongly suggests that the Cold Pool, a key oceanographic feature of the region, has waxed and waned across the continental shelf off the U.S. east coast consistent with known cold and warm periods in the past and produced the transgressions and regressions of the boreal community on the continental shelf herein exemplified by the ocean quahog (Fig. 3). The long-term history of the Cold Pool is not well understood, but the sensitivity of the regional footprint of the Cold Pool to recent warming temperatures is well described (Friedland et al., 2020a; 2022).

The occupation of the Delmarva inner continental shelf by ocean quahogs represents periods of transgression of habitable cold water inshore until conditions became unfavorable. The death assemblages produced contain a range of sizes and ages of animals, from small and young to large and old. Death assemblage compositions tend to be biased in favor of small (young) animals because the process of natural mortality usually adds a declining number of animals as the cohort ages and the individuals increase in size (Hallam, 1967; Cummins et al., 1986; Tomašových, 2004); whereas, taphonomic processes normally bias the assemblage against the preservation of the smallest size classes

(Staff et al., 1986; Powell and Stanton, 1996; Kidwell, 2001). Larger animals were selected for processing due to gear limitations, but the use of a lined dredge permitted routine collection of animals <20 years old so that the age distribution of the samples provides a good representation of the expected age distribution of the entire population at death except for the very youngest individuals; oldest ages >150 yr are consistent with the age range of present-day living populations (Hemeon et al., 2023a; 2023b; Sower et al., 2023a). Consequently, ages-at-death are likely older than an unbiased sampling of the entire size spectrum of the assemblage would otherwise provide, but a bias favoring young animals would still be anticipated by cohort mortality dynamics and despite the counterweighing bias of taphonomy, as these animals are young, but not necessarily small (Figs. 4–5). Consequently, increased numbers of animals at younger age would still be expected, and particularly as the most recent cohorts added to the death assemblage tend to be most numerous (Olszewski, 2004; Kosnik et al., 2009; Tomašových et al., 2014; 2018).

Surprisingly, the opposite was observed (Fig. 7). Considering the subfossil animals that lived contemporaneously with living animals (in the past 200 years), young animals become less common after approximately 120 years before present (Fig. 8). This shift in age distribution shows the age-at-death increasing through time with the animals of oldest age-at-death dying most recently, coinciding with the warm period during the 1930s–1950s and the 1960s–1970s cooling (Nixon et al., 2004; Bellucci et al., 2017; McClenachan et al., 2019). The few most recent new recruits observed in this study coincidentally date from this most recent period of cooling. The near absence of younger animals in the last 100 years of the timeseries overall, however, implies that recruitment decreased dramatically around 120 years ago, with the remaining deaths of older animals representing the slow demise of a non-recruiting population originally produced primarily by recruitment in the 19<sup>th</sup> century.

Older animals likely have a higher tolerance to high temperatures as a result of their ability to burrow deeper into the sediment (Taylor, 1976a; Ragnarsson and Thorarinsdottir, 2002; Strahl et al., 2011) to escape the higher temperatures that occur routinely in the Cold Pool when stratification breaks down in the fall before winter temperatures arrive. Temperature conditions similar to the annual maximum temperatures depicted in Fig. 8 result in a negative trend in growth and likely forecast a future cessation of growth, followed by death as higher temperatures remain for longer periods in the fall. Though direct observations are lacking, one might consider that survivorship would be very low for newly-settled animals under thermal conditions present through much of the 20<sup>th</sup> into the 21<sup>st</sup> century. This interpretation supports the conclusion that the times of death for recently dead shells collected off Delmarva are the product of an increase in bottom temperature that limited survivorship of newly-settled *A. islandica* followed by the eventual demise of the older animals as continuing yearly mortality took its toll.

The analysis of age-at-death depicted in Fig. 7 provides a unique mechanism that might be utilized to observe the rate of range recession in *A. islandica*. Unlike many bivalves, such as Atlantic surfclams (e.g., Narvaez et al., 2015), large ocean quahogs are less susceptible to increasing temperatures as a result of burrowing behavior that limits exposure to unfavorable conditions. Evidence of inshore range boundary recession for this species will likely be found first in the abundance of the juvenile animals in the population. Most importantly, evidence from the death assemblages sampled here strongly indicates that an *A. islandica* range shift on the trailing edge of the range is a 100+ year process rather than subdecadal as in many bivalve species such as the Atlantic surfclam (Jones et al., 2010; Hofmann et al., 2018; Baden et al., 2021). In this, the observed range of the ocean quahog in the Mid-Atlantic Bight may more closely reflect the range core of the past rather than present-day and more importantly obscure the ongoing effects of warming temperatures in the continuing presence of apparently robust populations wherein recruitment may have failed long ago.

## 5. Conclusions

Death assemblages are proving to be an important repository of information for the influence of climate change on the living community over timespans that exceed those of modern benthic surveys (Black et al., 2009; Wanamaker et al., 2009; Meadows et al., 2019; Powell et al., 2020). Ocean quahogs represent a long-term record of climate change on the U.S. northeast-coast continental shelf. This species transgressed and regressed across the shelf numerous times in accordance with cold and warm climatic periods. The growth rates of this species provide a unique view of climatic conditions during the times of occupation. Living ocean quahogs from multiple regions across the North-Atlantic shelf (Georges Bank, Long Island, New Jersey) were compared to subfossil shells collected from a region off Delmarva inshore of the present range. These populations exhibited different growth rates, with subfossil clams from Delmarva growing the fastest. Moreover, ocean quahog growth compared between regions and 20-year groupings from 1740 to 1940 showed both regional and temporal differences in growth, indicating that ocean quahogs that once occupied the inner-to-middle continental shelf off Delmarva continued to grow faster than animals from living populations taken from other regions throughout this timespan. Individuals representing each of the cold periods after the Holocene Climate Optimum, occupying the studied region off Delmarva, grew as fast or faster than individuals presently living in the Mid-Atlantic region probably due to optimal temperatures accompanied by increased food supply in shallow water. *Arctica islandica* growth changed throughout the Holocene, reflecting the changes in environmental conditions throughout the epoch with periods of the Neoglacial most closely representing modern-day growth rates suggestive of colder temperature conditions inshore during that time period.

Examining subfossil ocean quahogs from Delmarva with a shorter time-since-death, that is dying nearer present-day, the age range at death for ocean quahogs with the most recent radiocarbon birth dates was smaller than the age range for animals dying in the 1700s and 1800s, with clam births ceasing about 120 years ago. This trend describes the characteristics of range contraction offshore in *A. islandica* and strongly implicates diminishing recruitment and/or diminishing post-settlement survival about 120 years ago followed by the subsequent slow disappearance of live animals without replacement with the oldest dying most recently. Age-dependent mortality may be the product of the increased capability of older animals to burrow deeper than younger clams to escape high fall temperatures.

This is the largest spatial and temporal growth comparison of *A. islandica* ever recorded and the first record of the process by which this species' inshore range regresses as temperatures rise. Continuing to explore the relationship between the spatial and temporal difference in growth, birth, and age-at-death is important to interpret the current population dynamics of the *A. islandica* stock, to reconstruct the history of climate change in the Northwestern Atlantic during the Holocene and particularly the long-term dynamics of the Cold Pool, and to make future predictions as climate change continues.

## Declaration of competing interest

The authors declare that they have no known competing financial interests or personal relationships that could have appeared to influence the work reported in this paper.

## Acknowledgements

The authors would like to thank crew of the *F/V Betty C* for their assistance in collecting the samples and the use of their industry gear. The authors thank the National Marine Fisheries Service Northeast Fisheries Science Center (NEFSC) for making available the original datasets used in this study for site selection and we express particular appreciation of the efforts of the many individuals of the NEFSC survey

branch that participated in survey data collection over the 1980–2011 time period that made this study possible. This research was supported by the National Science Foundation (NSF) through the Industry/University Cooperative Research Center (I/UCRC) program supporting the Science Center for Marine Fisheries (SCEMFIS) under NSF awards 1841435 and 1841112 and through membership fees provided by the SCEMFIS Industry Advisory Board. Conclusions and opinions expressed herein are solely those of the authors.

## References

Appleyard, C.L., DeAlteris, J.T., 2001. Modeling growth of the northern quahog, *Mercenaria mercenaria*. *J. Shellfish Res.* 20, 1117–1125.

Auger, J.D., Mayewski, P.A., Maasch, K.A., Schuenemann, K.C., Carleton, A.M., Birkel, S.D., Saros, J.E., 2019. 2000 years of North atlantic-arctic climate. *Quat. Sci. Rev.* 216, 1–17.

Austad, S., 1996. The uses of intraspecific variation in ageing research. *Exp. Gerontol.* 31, 453–463.

Baden, S., Hernroth, B., Lindahl, O., 2021. Declining population of *Mytilus* spp. in North Atlantic coastal waters – a Swedish perspective. *J. Shellfish Res.* 40, 269–296.

Ballesta-Artero, I., Witbaard, R., Carroll, M.L., van der Meer, J., 2017. Environmental factors regulating gaping activity of the bivalve *Arctica islandica* in northern Norway. *Mar. Biol.* 164 (#116), 15.

Begum, S., Basova, L., Heilmayer, O., Philipp, E.E.R., Abele, D., Brey, T., 2010. Growth and energy budget models of the bivalve *Arctica islandica* at six different sites in the northeast Atlantic realm. *J. Shellfish Res.* 29, 107–115.

Begum, S., Abele, D., Brey, T., 2019. Toward the morphometric calibration of the environmental biorecorder. *Arctica islandica*. *J. Coast Res.* 35, 359–375.

Bellucci, A., Mariotti, A., Gualdi, S., 2017. The rate of forcings in the twentieth-century North Atlantic multidecadal variability: the 1940–75 North Atlantic cooling case study. *J. Clim.* 30, 7317–7337.

Black, B.A., Colbert, J.J., Pederson, N., 2008. Relationships between radial growth rates and lifespan within North American tree species. *Ecoscience* 15, 349–357.

Black, B.A., Copenheaver, C.A., Frank, D.C., Stuckey, M.J., Kormanyos, R.E., 2009. Multi-proxy reconstructions of northeastern Pacific geoduck. *Palaeogeogr. Palaeoclimatol. Palaeoecol.* 278, 40–47.

Brey, T., Voigt, M., Jenkins, K., Ahn, I.-Y., 2011. The bivalve *Laternula elliptica* at King George Island – a biological recorder of climate forcing in the West Antarctic Peninsula region. *J. Mar. Syst.* 88, 542–552.

Butler, P.G., Wanamaker Jr., A.D., Scourse, J.D., Richardson, C.A., Reynolds, D.J., 2013. Variability of marine climate on the North Icelandic Shelf in a 1357-year proxy archive based on growth increments in the bivalve *Arctica islandica*. *Palaeogeogr. Palaeoclimatol. Palaeoecol.* 373, 141–151.

Chen, Z., Curchitser, E., Chant, R., Kang, D., 2018. Seasonal variability of the cold Pool over the mid-atlantic Bight continental shelf. *J. Geophys. Res. Oceans* 123, 8203–8226.

Chen, Z., Curchitser, E.N., 2020. Interannual variability of the mid-atlantic Bight cold Pool. *J. Geophys. Res. Oceans* 125, e2020JC016445.

Chute, A.S., McBride, R.S., Emery, S.J., Robillard, E., 2016. Annulus formation and growth of Atlantic surfclam (*Spisula solidissima*) along a latitudinal gradient in the western North Atlantic Ocean. *J. Shellfish Res.* 35, 729–737.

Cummins, H., Powell, E.N., Stanton Jr., J.R., Staff, G., 1986. The size-frequency distribution in palaeoecology: the effects of taphonomic processes during formation of death assemblages in Texas bays. *Palaeontology* 29, 495–518.

Dahlgren, T.G., Weinberg, J.R., Halanych, K.M., 2000. Phylogeography of the ocean quahog (*Arctica islandica*): influences of paleoclimate on genetic diversity and species range. *Mar. Biol.* 137, 487–495.

Devillers, N., Eversole, A.G., Isely, J.J., 1998. A comparison of four growth models for evaluating growth of the northern quahog *Mercenaria mercenaria* (L.). *J. Shellfish Res.* 17, 191–194.

du Pontavice, H., Miller, T.J., Stock, B.C., Chen, Z., Saba, V.S., 2022. Ocean model-based covariates improve a marine fish stock assessment when observations are limited. *ICES J. Mar. Sci.* 79, 1259–1273.

du Pontavice, H., Chen, Z., Saba, V.S., 2023. A high-resolution ocean bottom temperature product for the northeast US continental shelf marine ecosystem. *Prog. Oceanogr.* 210, 102948.

Engelhart, S.E., Horton, B.P., Kemp, A.C., 2011. Holocene sea level change along the United States' Atlantic coast. *Oceanography* 24, 70–79.

Friedland, K.D., Mouw, C.B., Asch, R.G., Ferreira, S.A., Henson, S., Hyde, K.J.W., Morse, R.E., Thomas, A.C., Brady, D.C., 2018. Phenology and time series trends of the dominant seasonal phytoplankton bloom across global scales. *Global Ecol. Biogeogr.* 27, 551–569.

Friedland, K.D., Morse, R.E., Manning, J.P., Melrose, D.C., Miles, T., Goode, A.G., Brady, D.C., Kohut, J.T., Powell, E.N., 2020a. Trends and change points in surface and bottom thermal environments of the US northeast continental shelf ecosystem. *Fish. Oceanogr.* 29, 396–414.

Friedland, K.D., Morse, R.E., Shackell, N., Tam, J.C., Morano, J.L., Moisan, J.R., Brady, D.C., 2020b. Changing physical conditions and lower and upper trophic level responses on the US northeast shelf. *Front. Mar. Sci.* 7, #567445.

Friedland, K.D., Miles, T., Goode, A.G., Powell, E.N., Brady, D.C., 2022. The Middle Atlantic Bight Cold Pool is warming and shrinking: indices from *in situ* autumn seafloor temperatures. *Fish. Oceanogr.* 31, 217–223.

Hale, S.S., 2010. Biogeographical patterns of marine benthic macroinvertebrates along the Atlantic coast of the northeastern USA. *Estuar. Coast* 33, 1039–1053.

Hallam, A., 1967. The interpretation of size-frequency distributions in molluscan death assemblages. *Palaeontology* 10, 25–42.

Hemeon, K.M., Powell, E.N., Pace, S.M., Redmond, T.E., Mann, R., 2021a. Population dynamics of *Arctica islandica* at Georges Bank (USA): an analysis of sex-based demographics. *J. Mar. Biol. Assoc. U. K.* 101, 1003–1018.

Hemeon, K.M., Powell, E.N., Robillard, E., Pace, S.M., Redmond, T.E., Mann, R., 2021b. Attainability of accurate age frequencies for ocean quahogs (*Arctica islandica*) using large datasets: protocol, reader precision, and error assessment. *J. Shellfish Res.* 40, 255–267.

Hemeon, K.M., Powell, E.N., Pace, S.M., Mann, R., Redmond, T.E., 2023a. Population dynamics of *Arctica islandica* off Long Island (USA): an analysis of sex-based demographics and regional comparisons. *Mar. Biol.* 170 (3), 34.

Hemeon, K.M., Powell, E.N., Klinck, J.M., Mann, R., Pace, S.M., 2023b. Regional growth rates and growth synchronicity between two populations of *Arctica islandica* in the western Mid-Atlantic (US). *Estuar. Coast Shelf Sci.* 291, 108412.

Hofmann, E.E., Klinck, J.M., Kraeuter, J.N., Powell, E.N., Grizzle, R.E., Buckner, S.C., Bricej, V.M., 2006. A population dynamics model of the hard clam, *Mercenaria mercenaria*: development of the age- and length-frequency structure of the population. *J. Shellfish Res.* 25, 417–444.

Hofmann, E.E., Powell, E.N., Klinck, J.M., Munroe, D.M., Mann, R., Haidvogel, D.B., Narvaez, D.A., Zhang, X., Kuykendall, K.M., 2018. An overview of factors affecting distribution of the Atlantic surfclam (*Spisula solidissima*), a continental shelf biomass dominant, during a period of climate change. *J. Shellfish Res.* 37, 821–831.

Jones, D.S., Williams, D.F., Arthur, M.A., Krantz, D.E., 1984. Interpreting the paleo environmental, paleoclimatic and life history records in mollusc shells. *Geobios - Mem. Spec.* 8, 333–339.

Jones, S.J., Lima, F.P., Wethey, D.S., 2010. Rising environmental temperatures and biogeography: poleward range contraction of the blue mussel, *Mytilus edulis* L., in the western Atlantic. *J. Biogeogr.* 37, 2243–2259.

Kavanaugh, M.T., Rheubar, J.E., Luis, K.M., Doney, S.C., 2017. Thirty-three years of ocean benthic warming along the U.S. northeast continental shelf and slope: patterns, drivers, and ecological consequences. *J. Geophys. Res. Oceans* 122, 9399–9414.

Kidwell, S.M., 2001. Preservation of species abundance in marine death assemblages. *Science* 294, 1091–1094.

Kilada, R.W., Campana, S.E., Roddick, D., 2009. Growth and sexual maturity of the northern propellerclam (*Cyrtodaria siliqua*) in eastern Canada, with bomb radiocarbon age validation. *Mar. Biol.* 156, 1029–1037.

Killam, D.E., Clapham, M.E., 2018. Identifying the ticks of bivalve shell clocks: seasonal growth in relation to temperature and food supply. *Palaeo* 33, 228–236.

Kosnik, M.A., Hua, Q., Kaufman, D.S., Wüst, R.A., 2009. Taphonomic bias and time-averaging in tropical molluscan death assemblages: differential shell half-lives in Great Barrier Reef sediment. *Paleobiology* 35, 565–586.

Kraeuter, J.N., Ford, S., Cummings, M., 2007. Oyster growth analysis: a comparison of methods. *J. Shellfish Res.* 26, 479–491.

LeClaire, A.M., Powell, E.N., Mann, R., Hemeon, K.M., Pace, S.M., Sower, J.R., Redmond, T.E., 2022. Historical biogeographic range shifts and the influence of climate change on ocean quahogs (*Arctica islandica*) on the Mid-Atlantic Bight. *Holocene* 32 (9), 964–976.

Lellouche, J.-M., Greiner, E., Bourdalle-Badie, R., Garric, G., Melet, A., Drevillon, M., Bricaud, C., Harnon, M., Le Galloudec, O., Regnier, C., Candela, T., Testut, C.-E., Gasparin, F., Ruggiero, G., Benkiran, M., Yann, D., Le Traon, P.-Y., 2021. The Copernicus global 1/12 oceanic and sea ice GLORYS12 reanalysis. *Front. Earth Sci.* 9, 698876.

Lentz, S.J., 2017. Seasonal warming of the middle atlantic Bight cold Pool. *J. Geophys. Res. Oceans* 122, 941–954.

Lotze, H.K., Tittensor, D.P., Bryndum-Buchholz, A., Eddy, T.D., Cheung, W.W.L., Galbraith, E.D., Barange, M., Barrier, N., Bianchi, D., Blanchard, J.L., Bopp, L., Büchner, M., Bulman, C.M., Carozza, D.A., Christensen, V., Coll, M., Dunne, J.P., Fulton, E.A., Jennings, S., Jones, M.C., Mackinson, S., Maury, O., Niiranen, S., Oliveros-Ramos, R., Roy, T., Fernandes, J.A., Schewe, J., Shin, Y.-J., Silva, T.A.M., Steenbeek, J., Stock, C.A., Verley, P., Volkholz, J., Walker, N.D., Worm, B., 2019. Global ensemble projections reveal trophic amplification of ocean biomass declines with climate change. *Proc. Natl. Acad. Sci. USA* 116, 12907–12912.

Lucey, S.M., Nye, J.A., 2010. Shifting species assemblages in the northeast US continental shelf large marine ecosystem. *Mar. Ecol. Prog. Ser.* 415, 23–33.

Luquin-Cavarrubias, M.A., Morales-Bajorquez, E., Gonzalez-Palaez, S.S., Hidalgo-de-la-Toba, J.A., Lluch-Cota, D.E., 2016. Modeling of growth depensation of geoduck clam *Panope globosa* based on a multimodel inference approach. *J. Shellfish Res.* 35, 379–387.

McClenahan, L., Grabowski, J.H., Marra, M., McKeon, C.S., Neal, B.P., Record, N.R., Scyphers, S.B., 2019. Shifting perceptions of rapid temperature changes' effects on marine fisheries. *Fish. Fish.* 20, 1945–2017, 1111–1123.

McCuaig, J.M., Green, R.H., 1983. Unionid growth curves derived from annual rings: a baseline model for Long Point Bay, Lake Erie. *Can. J. Fish. Aquat. Sci.* 40, 436–442.

Meadows, C.A., Grebmeier, J.M., Kidwell, S.M., 2019. High-latitude benthic bivalve biomass and recent climate change: testing the power of live-dead discordance in the Pacific Arctic. *Deep-Sea Res. Pt. II Top. Stud. Oceanogr.* 162, 152–163.

Mette, M.J., Wanamaker Jr., A.D., Carroll, M.L., Ambrose Jr., W.G., Retella, M.J., 2016. Linking large-scale climate variability with *Arctica islandica* shell growth and geochemistry in northern Norway. *Limnol. Oceanogr.* 61, 748–764.

Mouw, C.B., Yoder, J.A., 2005. Primary production calculations in the Mid-Atlantic Bight including effects of phytoplankton community size structure. *Limnol. Oceanogr.* 50, 1232–1243.

Munroe, D.M., Powell, E.N., Mann, R., Klinck, J.M., Hofmann, E.E., 2013. Underestimation of primary productivity on continental shelves: evidence from maximum size of extant surfclam (*Spisula solidissima*) populations. *Fish. Oceanogr.* 22, 220–233.

Narvaez, D.A., Munroe, D.M., Hofmann, E.E., Klinck, J.M., Powell, E.N., Mann, R., Curchitser, E., 2015. Long-term dynamics in Atlantic surfclam (*Spisula solidissima*) populations: the role of bottom water temperature. *J. Mar. Syst.* 141, 136–148.

Nixon, S.W., Granger, S., Buckley, B.A., Lamont, M., Rowell, B., 2004. A one hundred and seventeen year coastal water temperature record from Woods Hole, Massachusetts. *Estuaries* 27, 397–404.

Oeschger, R., Storey, K.B., 1993. Impact of anoxia and hydrogen sulphide on the metabolism of *Arctica islandica* L. (Bivalvia). *J. Exp. Mar. Biol. Ecol.* 170, 213–226.

Olszewski, T.D., 2004. Modeling the influence of taphonomic destruction, reworking, and burial on time-averaging in fossil accumulations. *Palaeo* 19, 39–50.

Osman, M.B., Das, S.B., Trusel, L.D., Evans, M.I., Fischer, H., Grieman, M.M., Kipfahl, S., McConnell, J.R., Saltzman, E.S., 2019. Industrial-era decline in subarctic Atlantic productivity. *Nature* 569, 551–555.

Oviatt, C.A., 2004. The changing ecology of temperate coastal waters during a warming trend. *Estuaries* 27, 895–904.

Pace, S.M., Powell, E.N., Mann, R., Long, M.C., Klinck, J.M., 2017a. Development of an age–frequency distribution for ocean quahogs (*Arctica islandica*) on Georges Bank. *J. Shellfish Res.* 36, 41–53.

Pace, S.M., Powell, E.N., Mann, R., Long, M.C., 2017b. Comparison of age–frequency distributions for ocean quahogs *Arctica islandica* on the western Atlantic US continental shelf. *Mar. Ecol. Prog. Ser.* 585, 81–98.

Pace, S.M., Powell, E.N., Mann, R., 2018. Two-hundred-year record of increasing growth rates for ocean quahogs (*Arctica islandica*) from the northwestern Atlantic Ocean. *J. Exp. Mar. Biol. Ecol.* 503, 8–22.

Peherda, M., Walliser, E.O., Markulin, K., Purroy, A., Uvanovic, H., Janevic, I., Župan, I., Vilibic, I., Schöne, B.R., 2019. *Glycymeris pilosa* (Bivalvia) – a high-potential geochemical archive of the environmental variability in the Adriatic Sea. *Mar. Environ. Res.* 150, #104759.

Pershing, A.J., Alexander, M.A., Hernandez, C.M., Kerr, L.A., le Bris, A., Mills, K.E., Nye, J.A., Record, N.R., Scannell, H.A., Scott, J.D., Sherwood, G.D., Thames, A.C., 2015. Slow adaptation in the face of rapid warming leads to collapse of the Gulf of Maine cod fishery. *Science* 350, 809–812.

Peterson, C.H., Duncan, P.B., Summerson, H.C., Beal, B.F., 1985. Annual band deposition within shells of the hard clam, *Mercenaria mercenaria*: consistency across habitat near Cape Lookout, North Carolina. *Fish. Bull.* 88, 671–677.

Poussard, L.M., Powell, E.N., Hennen, D.R., 2021. Discriminating between high- and low-quality field depletion experiments through simulation analysis. *Fish. Bull.* 119, 274–293.

Powell, E.N., Stanton Jr., R.J., 1996. The application of size-frequency distribution and energy flow in paleoecologic analysis: an example using paraautochthonous death assemblages from a variable salinity bay. *Palaeogeogr. Palaeoclimatol. Palaeoecol.* 124, 195–231.

Powell, E.N., Ewing, A.M., Kuykendall, K.M., 2020. Ocean quahogs (*Arctica islandica*) and Atlantic surfclams (*Spisula solidissima*) on the Mid-Atlantic Bight continental shelf and Georges Bank: the death assemblage as a recorder of climate change and the reorganization of the continental shelf benthos. *Palaeogeogr. Palaeoclimatol. Palaeoecol.* 537, 16. #109205.

R Core Team, 2021. R: A Language and Environment for Statistical Computing. R Foundation for Statistical Computing, Vienna, Austria. URL <https://www.R-project.org/>.

Ragnarsson, S.A., Thorarinsdottir, G.G., 2002. Abundance of ocean quahog, *Arctica islandica*, assessed by underwater photography and a hydraulic dredge. *J. Shellfish Res.* 21, 673–676.

Ren, J.S., Ross, A.H., 2001. A dynamic energy budget model of the Pacific oyster *Crassostrea gigas*. *Ecol. Model.* 142, 105–120.

Reynolds, D.J., Richardson, C.A., Scourse, J.D., Butler, P.E., Hollyman, P., Poman-Gonzalez, A., Hall, I.R., 2017. Reconstructing North Atlantic marine climate variability using an absolutely-dated sclerochronological network. *Palaeogeogr. Palaeoclimatol. Palaeoecol.* 465, 333–346.

Richardson, C.A., 2001. Molluscs as archives of environmental change. *Oceanogr. Mar. Biol. Annu. Rev.* 39, 103–164.

Richardson, A.J., Schoeman, D.S., 2004. Climate impact on plankton ecosystems in the northeast Atlantic. *Science* 303, 160–163.

Ridgway, I.D., Richardson, C.A., Austad, S.N., 2011. Maximum shell size, growth rate, and maturation age correlate with longevity in bivalve molluscs. *J. Gerontol. Ser. A: Biomedical Sci. Medical Sci.* 66, 183–190.

Saba, V.S., Griffies, S.M., Anderson, W.G., Winton, M., Alexander, M.A., Delworth, T.L., Hare, J.A., Harrison, M.J., Rosati, A., Vecchi, G.A., Zhang, R., 2016. Enhanced warming of the northwest Atlantic Ocean under climate change. *J. Geophys. Res. Oceans* 121, 118–132.

Schöne, B.R., Houk, S.D., Freyre Castro, A.D., Fiebig, J., Oschmann, W., Kröncke, I., Dreyer, W., Gosselk, F., 2005. Daily growth rates in shells of *Arctica islandica*: assessing sub-seasonal environmental controls on a long-lived bivalve mollusk. *Palaeo* 20, 78–92.

Seidov, D., Baranova, O.K., Boyer, T.P., Cross, S.L., Mishonov, A.V., Parsons, A.R., 2016. Northwest Atlantic regional ocean climatology. *Bull. Am. Meterol. Soc.* 99, 2129–2138.

Shchepetkin, A.F., McWilliams, J.C., 2005. The regional oceanic modeling system (ROMS): a split-explicit, free-surface, topography-following-coordinate oceanic model. *Ocean Model.* 9, 347–404.

Shirai, K., Kubota, K., Murakami-Sugihara, N., Seike, K., Hakozaiki, M., Tanabe, K., 2018. Stimpson's hard clam *Mercenaria stimpsoni*: a multi-decadal climate recorder for the northeast Pacific coast. *Mar. Environ. Res.* 133, 49–56.

Sower, J.R., Robillard, E., Powell, E.N., Hemeon, K.M., Mann, R., 2022. Defining patterns in ocean quahog (*Arctica islandica*) sexual dimorphism along the Mid-Atlantic Bight. *J. Shellfish Res.* 41, 335–348.

Sower, J.R., Powell, E.N., Mann, R., Hemeon, K.M., Pace, S.M., Redmond, T.E., 2023a. Examination of spatial heterogeneity in population age frequency and recruitment in the ocean quahog (*Arctica islandica Linnaeus 1767*). *Mar. Biol.* 170 (4), 38.

Sower, J.R., Powell, E.N., Hemeon, K.M., Mann, R., Pace, S.M., 2023b. Ocean quahog (*Arctica islandica*) growth rate analyses of four populations from the Mid-Atlantic Bight and Georges Bank. *Continent. Shelf Res.* 265, 105076.

Solidoro, C., Pastres, R., Canu, D.M., Pellizzato, M., Rossi, R., 2000. Modelling the growth of *Tapes philippinarum* in northern Adriatic lagoons. *Mar. Ecol. Prog. Ser.* 199, 137–148.

Staff, G.M., Stanton Jr., R.J., Powell, E.N., Cummins, H., 1986. Time-averaging, taphonomy and their impact on paleocommunity reconstruction: death assemblages in Texas bays. *Geol. Soc. Am. Bull.* 97, 428–443.

Strahl, J., Brey, T., Philipp, E.E.R., Thorarinsdottir, G., Fischer, N., Wessels, W., Abele, D., 2011. Physiological responses to self-induced burrowing and metabolic rate depression in the ocean quahog *Arctica islandica*. *J. Exp. Biol.* 214, 4223–4233.

Tanaka, M., 1982. A new growth curve which expresses infinite increase. *Amakusa Mar. Biol. Lab.* 6, 167–177.

Tanaka, M., 1988. Eco-physiological meaning of parameters of ALOG growth curve. *Amakusa Mar. Biol. Lab.* 9, 103–106.

Taylor, A.C., 1976a. Burrowing behaviour and anaerobiosis in the bivalve *Arctica islandica* (L.). *J. Mar. Biol. Assoc. U. K.* 56, 95–109.

Taylor, A.C., 1976b. The cardiac responses to shell opening and closure in the bivalve *Arctica islandica* (L.). *J. Exp. Biol.* 64, 751–759.

Tomašových, A., 2004. Postmortem durability and population dynamics affecting the fidelity of brachiopod size-frequency distributions. *Palaios* 19, 477–496.

Tomašových, A., Kidwell, S.M., Barber, R.F., Kaufman, D.S., 2014. Long-term accumulation of carbonate shells reflects a 100-fold drop in loss rate. *Geology* 42, 819–822.

Tomašových, A., Gallmetzer, I., Haselmair, A., Kaufman, D.S., Kralj, M., Cassin, D., Zonta, R., Zuschin, M., 2018. Tracing the effects of eutrophication on molluscan communities in sediment cores: outbreaks of an opportunistic species coincide with reduced bioturbation and high frequency of hypoxia in the Adriatic Sea. *Paleobiology* 44, 575–602.

Vihtakari, M., Renaud, P.E., Clarke, L.J., Whitehouse, M.J., Hop, H., Carroll, M.L., Ambrose Jr., W.G., 2016. Decoding the oxygen isotope signal for seasonal growth patterns in Arctic bivalves. *Palaeogeogr. Palaeoclimatol. Palaeoecol.* 446, 263–283.

Wanamaker Jr., A.D., Kreutz, K.J., Schöne, B.R., Maasch, K.A., Pershing, A.J., Burns, H. W., Intione, D.S., Feindel, S., 2009. A late Holocene paleo-productivity record in the western Gulf of Maine, USA, inferred from growth histories of the long-lived ocean quahog (*Arctica islandica*). *Int. J. Earth Sci.* 98, 19–29.

Wanamaker Jr., A.D., Kreutz, K.J., Schöne, B.R., Intone, D.S., 2011. Gulf of Maine shells reveal changes in seawater temperature seasonality during the medieval climate anomaly and the little ice age. *Palaeogeogr. Palaeoclimatol. Palaeoecol.* 302, 47–51.

Wanner, H., Solomina, O., Grosjean, M., Ritz, S.P., Jetal, M., 2011. Structure and origin of Holocene cold events. *Quat. Sci. Rev.* 30, 3109–3123.

Witbaard, R., 1996. Growth variations in *Arctica islandica* L. (Mollusca): a reflection of hydrography-related food supply. *ICES J. Mar. Sci.* 53, 981–987.

Witbaard, R., Bergman, M.J.N., 2003. The distribution and population structure of the bivalve *Arctica islandica* L. in the North Sea: what possible factors are involved? *J. Sea Res.* 50, 11–25.

Wood, S.N., 2011. Fast stable restricted maximum likelihood and marginal likelihood estimation of semiparametric generalized linear models. *J. Roy. Stat. Soc. B* 73, 3–36.

Woodin, S.A., Hilbish, T.J., Helmuth, B., Jones, S.J., Wethey, D.S., 2013. Climate change, species distribution models, and physiological performance metrics: predicting when biogeographic models are likely to fail. *Ecol. Evol.* 3, 3334–3346.

Yoder, J.A., Schollaert, S.E., O'Reilly, J.E., 2002. Climatological phytoplankton chlorophyll and sea surface temperature patterns in continental shelf and slope water off the northeast U.S. coast. *Limnol. Oceanogr.* 47, 672–682.

Zettler, M.L., Bönsch, R., Gosselck, F., 2001. Distribution, abundance and some population characteristics of the ocean quahog, *Arctica islandica* (Linnaeus, 1767), in the Mecklenburg Bight (Baltic Sea). *J. Shellfish Res.* 20, 161–169.